

A Novel Method to Probe the Pronounced Growth of Correlation Lengths in an Active Glass-forming Liquids using Elongated Probe

Anoop Mutneja ¹, and Smarajit Karmakar ¹

¹ *Tata Institute of Fundamental Research, 36/P, Gopanpally Village,
Serilingampally Mandal, Ranga Reddy District, Hyderabad, Telangana 500107, India*

The growth of correlation lengths in equilibrium glass-forming liquids near the glass transition is considered a critical finding in the quest to understand the physics of glass formation. These understandings helped us understand various dynamical phenomena observed in supercooled liquids. It is known that at least two different length scales exist - one is of thermodynamic origin, while the other is dynamical in nature. Recent observations of glassy dynamics in biological and synthetic systems where the external or internal driving source controls the dynamics, apart from the usual thermal noise, led to the emergence of the field of active matter. A question of whether the physics of glass formation in these active systems is also accompanied by growing dynamic and static lengths is indeed timely. In this article, we probe the growth of dynamic and static lengths in a model active glass system using rod-like elongated probe particles, an experimentally viable method. We show that the dynamic and static lengths in these non-equilibrium systems grow much more rapidly than their passive counterparts. We then offer an understanding of the violation of the Stokes-Einstein relation and Stokes-Einstein-Debye relation using these lengths via a scaling theory.

One of the fascinating properties exhibited by the supercooled liquids is the existence of local patches with heterogeneous dynamical properties, known as dynamic heterogeneity (DH) in the literature [1]. Many observed properties like stretched exponential relaxation, breakdown of Stokes-Einstein (SE) relation, non-Gaussian Van Hove function, etc., can be attributed to the existence of DH [1–3]. In recent decades, numerous computer simulations and experimental studies have linked a growing dynamic length (ξ_d) with DH [2, 4]. There are various methods to compute dynamic length in computer simulations. Doing finite size scaling (FSS) of observables linked to DH, e.g. the four-point dynamical susceptibility $\chi_4(t)$ [5], Binder cumulant of Van Hove function [3, 6] etc, is one such popular method. Another elegant method is block analysis in which scaling analysis is done in a subsystem [6, 7]. Block analysis also has certain advantages over the traditional FSS, like the inclusions of number, concentrations, temperature, and other possible fluctuations that are absent in the usual FSS, improved statistics, the need for only one large system size, etc. The most important advantage is its applicability in colloidal experiments. At the same time, it is essential to highlight that it is still challenging to reach the degree of supercooling attainable in real molecular liquids via computer simulations, even with the recent technique of swap Monte-Carlo [8]. Thus although simulations and colloidal experiments are very important in the quest to understand the physics of glass transition, appropriate experimental studies on molecular glasses are essential.

Another length that comes up while studying various thermodynamic properties of supercooled liquids is often referred to as the “Mosaic scale” (ξ_s) in the random first-order transition theory (RFOT) of glass transition [9, 10]. In simulations, static length can be obtained via FSS of the minimum eigenvalue of a configuration’s Hessian ma-

trix [11] computed in the energy-minimized inherent state or via the point-to-set (PTS) method [12], or by FSS of the characteristic relaxation time, τ_α (see Supplementary Material), [5]. This length, ξ_s , grows more slowly than ξ_d , suggesting a possible different origin. Thus obtaining the length scales in experimentally relevant glass-forming liquids will certainly be a major advancement in developing an unified theory of glass formation.

Measuring growing lengths in experimental systems is extremely difficult. The computer simulations have the liberty to track the position of each particle to obtain detailed microscopic information. In contrast, the same cannot be done in actual molecular liquids, where the supercooling effects are enormous to emphasize again. There are indirect experimental procedures where people have obtained these length scales [13–15], but they are undoubtedly challenging. Recently, there has been a successful effort to get the static length scale by studying the change in the dielectric relaxation in supercooled glycerol in the presence of a larger size cosolute particle (sorbitol in this case) [16]. In Refs. [4, 17, 18], we proposed a novel method to obtain both ξ_d and ξ_s by studying the effect of supercooling on the dynamics of different-sized elongated probe particles. The motivation behind doing the same is twofold. The first is its experimental feasibility. The vast literature on single-molecule experiments backs that up [19–25]. Secondly, doing FSS in experiments is tricky, while the external probes of different sizes would give us dynamical information at different coarse-grained lengths, hence serving our purpose.

The discovery of glass-like behaviour in various biological systems where the internal source of energy and not the thermal fluctuations dictates the system’s dynamical evolution leads to the emergence of a new field of research known as active matter. In these systems, the driving forces in constituent elements or particles often come

from internal energy dissipation (self-propulsion) or external driving. Thus they are inherently non-equilibrium in nature. The dynamical behaviour of these systems in their stationary states (non-equilibrium steady states) is of significant current interest due to its relevance in various systems. The wound healing phenomenon, dynamics inside the cytoplasm [26, 27], flocking and migratory behaviour of animals, birds, insects etc., as well as synthetic Janus colloidal assemblies, driven granular fluid [28] etc., are a few examples of active matter systems. Many analytical and numerical models [29–39] have been studied within the broad framework of statistical mechanics to understand the emergent cooperative behaviour of these active matter systems both in dilute and dense limits. Recently, Paul et al. [40] studied such an active glass model via extensive large-scale simulations and showed a dramatic five-fold or more increase in the dynamic length scale compared to a similar passive system. This massive increase in the DH in the presence of active particles is also experimentally observed [26–28]. In [40], all the existing methods to obtain ξ_d are employed to show that a unique dynamic length scale controls the dynamics. Thus this system is an interesting model to check whether the same length can be probed by looking at the rotational and translational dynamics of a rod-like probe particle with the ambition of its subsequent use in ubiquitous out-of-equilibrium experimental situations.

In this work, we studied an active glass model, which has recently been studied extensively [40, 41] to understand the effect of non-equilibrium active forces on the phenomena of glass transition. We simulated a binary glass-forming liquid known as the Kob-Andersen model[42]. The system contains the larger (A type) and smaller (B type) point particles in an 80:20 ratio. We studied a system with $N = 50000$ particles, out of which $N_a = 0.1N$ of particles are chosen randomly to be active particles. These particles follow run-and-tumble motion with the persistence time of $\tau_p = 1.0$ in the Lennard-Jones unit. The system is studied in the temperature range $T \in [0.340 - 2.00]$. In each simulation, $N_r = 20$ probe rods are introduced and their position, r_{cm} and orientation, \hat{u} are evolved via Newtonian dynamics. Further model and simulation details can be found in the Supplementary Materials (SM).

Heterogeneity in the dynamics can be quantified via the Van Hove function ($G(r(t^*))$), which is the distribution of displacement of particles, $r(t^*)$ during a time interval t^* . In supercooled liquids, it is known that the Van Hove function has exponential tails on top of the usual Gaussian core owing to DH. The exponential tails correspond to the hopping process in the supercooled liquid. A similar correlation function for the rotational degrees of freedom is not Gaussian but is the solution to a

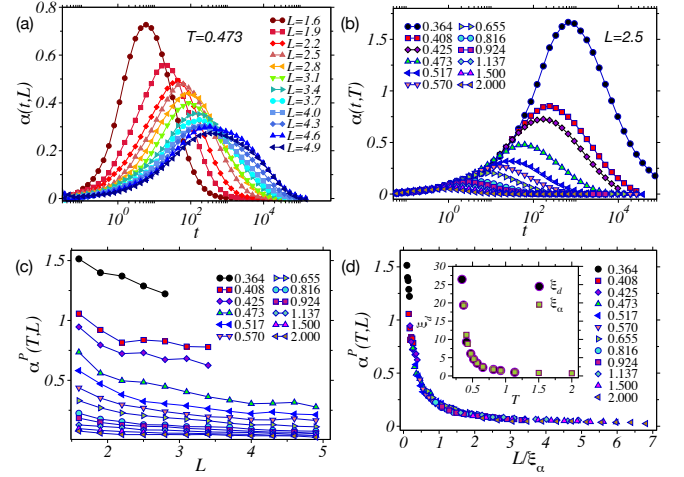


FIG. 1. (a) Time evolution of the non-normal parameter $\alpha(t, L)$ (Eq:2) is plotted for rods of variable sizes in supercooled system ($T = 0.473$). (b) Temperature variation in the time evolution of $\alpha(t, T)$ for rod of length $L = 2.5$. (c) Rod length dependence of the peak height of $\alpha(t)$ for different supercooling temperatures. The increase in $\alpha^P(T, L)$ with decreasing temperature and rod length signifies the length scale picked up by the rod dynamics. (d) The peak heights of panel (c) are collapsed using a scaling relation (see text) to obtain the length scale ξ_α . The obtained length scale grows by the enormous factor of twenty, and is shown in the inset, along with the comparison with the numbers from Ref.[40].

three-dimensional rotational diffusion equation, as

$$G(\theta(t^*)) = \sum_{n=0}^{\infty} \frac{2n+1}{2} \mathcal{P}_n(\cos(\theta)) e^{-n(n+1)D_r t^*}. \quad (1)$$

Here $\cos(\theta(t^*)) = \hat{u}(t^*) \cdot \hat{u}(0)$, \mathcal{P}_n is n th order Legendre polynomials, and D_r is the rotational diffusion constant of the rod. With this solution in hand, one can compute a Non-Normal parameter $\alpha(t, T, L)$ as

$$\alpha(t) = \frac{1}{2} \frac{\langle |\hat{u}(t) - \hat{u}(0)|^4 \rangle}{(\langle |\hat{u}(t) - \hat{u}(0)|^2 \rangle)^2} + \frac{1}{6} \langle |\hat{u}(t) - \hat{u}(0)|^2 \rangle - 1 \quad (2)$$

For a rod in a supercooled liquid, one expects $\alpha(t)$ to peak at the time close to τ_α and eventually go to zero for large times. Fig.2(b) shows the time evolution of the non-normal parameter at various parent liquid temperatures. Also, for a given supercooling, the effect of DH on the rotational dynamics of the rod would dwindle with an increase in rod length because of the increased spatial average. Fig.2(a) depicts the same. The peak height α^P is indeed found to be a good measure for obtaining the dynamic heterogeneity length of the parent liquid [17] via scaling analysis at equilibrium. Assuming it to be true even for these non-equilibrium steady states, we performed a detailed scaling analysis of α^P as a function of increasing rod length in our active glass model. Note that α^P should also go to zero in the large

rod length limit, so there is just one scaling parameter, the length scale ξ_α . Fig.2(c) shows the rod length dependence of $\alpha^P(T, L)$ for different temperatures, and on assuming the scaling form of $\alpha^P(T, L) = \mathcal{F}(L/\xi_\alpha(T))$, one can collapse the data to a master curve. This collapse is shown in Fig.2(d), along with the comparison of obtained length scale to the dynamic length scale of the system obtained from various other methods (from paper [40]). The remarkable agreement of our results with previously reported one, clearly establishes the robustness of the proposed method in out-of-equilibrium active glasses using elongated probe particles. We hope that future experiments will use this method to measure these correlations in active glassy systems of experimental relevance.

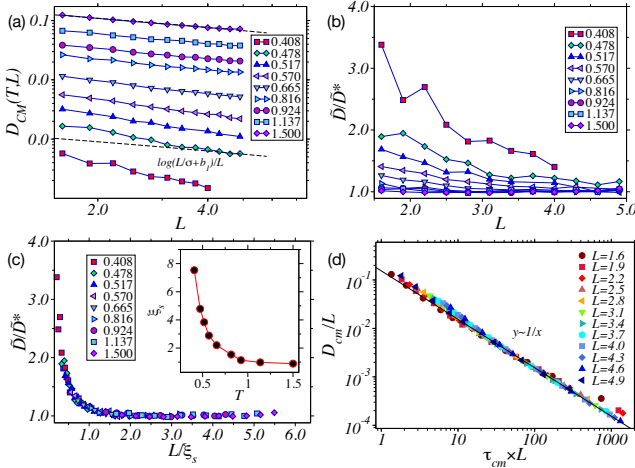


FIG. 2. (a) The rod length variation of the diffusion constant of CoM of rod in system at different temperatures. The supercooling effects can be seen from the deviation from dotted lines ($D_{cm} \sim \ln(L/\sigma + b_1)/L$). (b) To quantify the deviation, $\tilde{D} = D_{cm}L/\ln(L/\sigma + b_1)$, scaled by its large rod length limit, \tilde{D}^* is plotted against the rod length. The variation clearly suggest the length scale involved. (c) Data collapse is shown by using the static length scale of the system. (used from ref.[41]) (d) D_{cm} and τ_{cm} follows the inverse relation, thus similar analysis can be performed on τ_{cm} , and is presented in SM.

After studying the rotational dynamics of the probe particles, we now focus on the translational dynamics of the probes. We have calculated the diffusion constant (D_{cm}) and the translational relaxation time (τ_{cm}) of the centre of mass (CoM) of the probes. It is known that the translational diffusion constant (D_{cm}) of a Brownian rod should decrease with increasing rod length as $D_{cm} \sim \ln(L/\sigma + b_1)/L$, while the relaxation time follows the inverse relation $\tau_{cm} \sim L/\ln(L/\sigma + b_2)$ [43]. Here $\sigma = 1.0$ is the rod width, and b_1, b_2 are different constants to consider the hydrodynamic interactions. The fitted dotted line in Fig.2(a) shows the validation of the same for large temperatures ($T = 1.5$). One can immediately see the deviation from this behaviour

with increasing supercooling. The shorter rods tend to move faster than they should have, based on the trend in the large rod limit. To quantify the same we studied $\tilde{D} = D_{cm}L/\ln(L/\sigma + b_1)$ as shown in Fig.2(b). Note that the y-axis variation is scaled by large rod length limit \tilde{D}^* . On decreasing the temperature, the variables \tilde{D}/\tilde{D}^* show stronger deviation from $\tilde{D}/\tilde{D}^* = 1$ for smaller rods. This suggests that an inherent length scale must be controlling these effects, and one should be able to collapse the data to master curves by assuming the scaling relations $\tilde{D}/\tilde{D}^*(L, T) = \mathcal{F}(L/\xi_{D_{cm}}(T))$. The collapse obtained in Fig.2(c) is indeed very good and the length obtained closely follows the temperature variation of the static length scale reported in Ref.[41]. This suggests that the method is very robust in obtaining static correlation length even in a non-equilibrium system. Moreover, this method has the benefit of only requiring the mean translational diffusion constant or the relaxation time of the probes of different lengths at different temperatures. Existing results in the literature [19–25] clearly suggests that these measurements are not very difficult in real experiments. Since the D_{cm} and τ_{cm} follows the inverse relation (Fig.2(d)), similar analysis can be performed on τ_{cm} , and is presented in SM.

Next, we study the Stokes-Einstein (SE) and Stokes-Einstein-Debye (SED) violations in these systems and show how the physics of SE and SED breakdown can be understood using the same correlation lengths in a unified manner. SE violation is a hallmark of DH. SE relation combines the two dynamic phenomena, namely diffusion and drag, and it reads as $D_s\eta/T = \text{const.}$. Here D_s is the self-diffusion constant, and η is the medium's viscosity. The SE relation equates the two relaxation times, the diffusive R^2/D_s , and the viscous $\eta R^3/T$, up to a constant factor. While in supercooled liquids, it breaks down because different phenomena control different time scales. More mobile particles control the diffusive time scale, while the slower set controls the viscous time scale. Thus, more DH in the system would lead to stronger violations in the SE relation.

The idea of obtaining SEB temperature at various length scales was studied originally in the reference [44]. It was found that if one computes the wave-vector-dependent relaxation time, then there exists a critical wave-vector at each temperature below which the SE relation will be obeyed. This critical wave-vector at each temperature turns out to be uniquely related to the inverse of the dynamic heterogeneity length scale. A similar crossover is obtained if one studies the SE relation for elongated rod-like probe particles with changing probe lengths. This idea was successfully used in Ref.[18] to obtain the largest temperature where SEB happens for a particular rod length, and then the corresponding dynamic length could be extracted.

Taking relaxation time is taken as a proxy for viscosity, the SE relation can be rephrased as, $D\tau = \frac{f(R, T)}{\pi R}$,

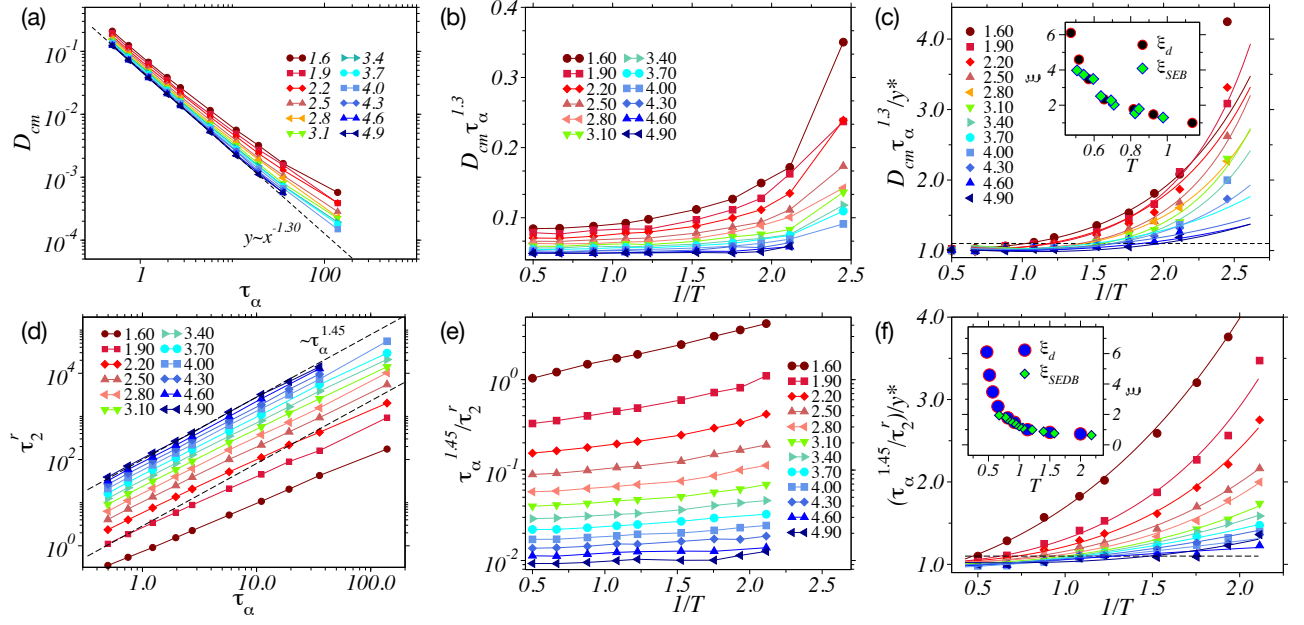


FIG. 3. (a) Diffusion constant of rod's CoM (D_{cm}) shows a power law dependence against τ_α of the medium with the power of -1.30 . Shorter rods tend to deviate from this power-law with increasing supercooling (b) The SE parameter, $D_{cm}\tau_\alpha^{1.30}$ is plotted against inverse temperature for different rod sizes. The SEB can be seen to be happening at higher temperatures for smaller rods. (c) The SE parameter scaled by the large T limit is plotted as symbols in main panel. The lines are the fit of these points via function $y = y^* \exp[x + c_0(x/x_0)^n + c_1(x/x_0)^{2n}]$, and SEB temperature is determined as $y/y^* = 1.1$ cut. The SEB temperature for different rod lengths is compared with the dynamic length scale of the system in the inset. (d, e, f) Similar analysis shown is for the Stokes-Einstein-Debye (SED) relation using the rotational relaxation time (τ_2^r) of the probe rods.

where R would be the effective hydrodynamic radius of the probe rod and $f(R, T)$ would act as a Stokes-Einstein breakdown (SEB) parameter. From Fig.2(d), we know that the relaxation time and diffusion constant related to CoM obey the SE relation, but if one considers the diffusion of a rod with respect to the medium's relaxation times, then SE is found to be violated. Fig.3(a) shows the plot of D_{cm} versus τ_α . The larger rods obey a modified SE relation as $D_{cm}\tau_\alpha^{1.3} = \text{const.}$, where the exponent 1.3 is not apriori clear to us. Now, if we plot the SEB parameter ($D_{cm}\tau_\alpha^{1.3}$) for rods of different sizes (Fig.3(b)), then we will be able to obtain the temperature where the breakdown happens. To get the same, we scaled the parameter, $D_{cm}\tau_\alpha^{1.3}(T, L)$ by $y^* = D_{cm}\tau_\alpha^{1.3}(T = 1.5, L)$ and plotted it against the inverse temperature as shown in the main panel of Fig.3(c). One can see the violation of SE relation happening at lower and lower temperatures with increasing rod size. The breakdown temperature corresponding to $D_{cm}\tau_\alpha^{1.3}(T, L)/y^* = 1.1$ for each rod length is taken to be the SEB temperature. The symbols in Fig.3(c) were fitted to a function $y = y^* \exp[x + c_0(x/x_0)^n + c_1(x/x_0)^{2n}]$ (solid lines in Fig.3(c)), to correctly obtain the SEB temperature. The obtained SEB temperature plotted against rod length is then compared to the dynamic length of the parent liquid in the inset of Fig.3(c). The two lengths match very well, providing another way to obtain the dynamic length

from the SE violation of a probe particle. Similarly, for the rotational dynamics of the rods, one can check the Stokes-Einstein-Debye (SED) relation. Fig.3(d) shows the rotational relaxation (τ_2^r , see the definition in SM) time against the τ_α . They follow $\tau_2^r \tau_\alpha^{1.45}$ power law relation in high-temperature and large rod length limit. Note again the origin of the exponent, 1.45 is not immediately known. But, $\tau_\alpha^{1.45}/\tau_2^r$ can then be considered as the SED breakdown (SEDB) parameter. SEDB is shown in Fig.3(e) against inverse temperature. After scaling it with the $T = 1.5$ value, one can see the SEDB happening at lower temperatures for larger rods (Fig.3(f)). The SEDB temperatures are then obtained at $\tau_\alpha^{1.45}/\tau_2^r/y^* = 1.1$ cut. The obtained length ξ_{SEDB} is compared with the dynamic length of the system in the inset. Again the very good comparison with the dynamical heterogeneity length immediately tells us that all these phenomena are uniquely controlled by the same length scale. Moreover SEB and SEDB can then be a good measure to obtain the underlying growth of the dynamic length scale.

Finally, to conclude, we have obtained the dynamic and static correlation lengths in an active model glass-forming liquids using elongated probe particles and show how the rotational dynamics of the probe can capture the dramatic growth of the dynamic correlation length, thereby opening a new avenue to obtain the same corre-

lation length in various experimental systems including biological systems where glassy dynamics are found to be ubiquitous. Similarly, the information of the static length scale using our scaling theory will surely help us in the near future to extend the physics of glass transition and the role of various correlation lengths in non-equilibrium systems with similar dynamical behaviour. In the end, we show how the physics of Stokes-Einstein and Stokes-Einstein-Debye breakdown can be understood using these correlation lengths, as well as how violation of SE and SEB can be elegantly used to even obtain the underlying correlation lengths via an unified scaling analysis. We hope these results will encourage future experimental measurements in these non-equilibrium active matter systems to probe the growth of correlations and help unearth the rich physics of glass transition in a wide variety of systems in equilibrium and non-equilibrium situations.

We acknowledge the support of the Department of Atomic Energy, Government of India, under Project Identification No. RTI 4007. SK acknowledges support from Core Research Grant CRG/2019/005373 from Science and Engineering Research Board (SERB) and Swarna Jayanti Fellowship grants DST/SJF/PSA-01/2018-19 and SB/SFJ/2019-20/05.

-
- [1] L. Berthier, G. Biroli, J.-P. Bouchaud, L. Cipelletti, and W. van Saarloos, eds., *Dynamical Heterogeneities in Glasses, Colloids, and Granular Media* (Oxford University Press, 2011).
 - [2] S. Karmakar, C. Dasgupta, and S. Sastry, Length scales in glass-forming liquids and related systems: a review, *Reports on Progress in Physics* **79**, 016601 (2015).
 - [3] P. Chaudhuri, L. Berthier, and W. Kob, Universal nature of particle displacements close to glass and jamming transitions, *Phys. Rev. Lett.* **99**, 060604 (2007).
 - [4] I. Tah, A. Mutneja, and S. Karmakar, Understanding Slow and Heterogeneous Dynamics in Model Supercooled Glass-Forming Liquids, *ACS Omega* **6**, 7229 (2021).
 - [5] S. Karmakar, C. Dasgupta, and S. Sastry, Growing length and time scales in glass-forming liquids, *Proceedings of the National Academy of Sciences* **106**, 3675 (2009), <https://www.pnas.org/content/106/10/3675.full.pdf>.
 - [6] B. P. Bhowmik, I. Tah, and S. Karmakar, Non-gaussianity of the van hove function and dynamic-heterogeneity length scale, *Physical Review E* **98**, 10.1103/physreve.98.022122 (2018).
 - [7] S. Chakrabarty, I. Tah, S. Karmakar, and C. Dasgupta, Block analysis for the calculation of dynamic and static length scales in glass-forming liquids, *Phys. Rev. Lett.* **119**, 205502 (2017).
 - [8] L. Berthier, E. Flenner, C. J. Fullerton, C. Scalliet, and M. Singh, Efficient swap algorithms for molecular dynamics simulations of equilibrium supercooled liquids, *Journal of Statistical Mechanics: Theory and Experiment* **2019**, 064004 (2019).
 - [9] T. R. Kirkpatrick, D. Thirumalai, and P. G. Wolynes, Scaling concepts for the dynamics of viscous liquids near an ideal glassy state, *Phys. Rev. A* **40**, 1045 (1989).
 - [10] V. Lubchenko and P. G. Wolynes, Theory of structural glasses and supercooled liquids, *Annual Review of Physical Chemistry* **58**, 235 (2007).
 - [11] G. Biroli, S. Karmakar, and I. Procaccia, Comparison of static length scales characterizing the glass transition, *Phys. Rev. Lett.* **111**, 165701 (2013).
 - [12] G. Biroli, J.-P. Bouchaud, A. Cavagna, T. S. Grigera, and P. Verrocchio, Thermodynamic signature of growing amorphous order in glass-forming liquids, *Nature Physics* **4**, 771 (2008).
 - [13] S. Albert, T. Bauer, M. Michl, G. Biroli, J.-P. Bouchaud, A. Loidl, P. Lunkenheimer, R. Tourbot, C. Wiertel-Gasquet, and F. Ladieu, Fifth-order susceptibility unveils growth of thermodynamic amorphous order in glass-formers, *Science* **352**, 1308 (2016).
 - [14] L. Berthier, G. Biroli, J.-P. Bouchaud, L. Cipelletti, D. E. Masri, D. L'Hôte, F. Ladieu, and M. Pierno, Direct Experimental Evidence of a Growing Length Scale Accompanying the Glass Transition, *Science* **310**, 1797 (2005), [cond-mat/0512379](https://doi.org/10.1126/science.1123799).
 - [15] A. S. Keys, A. R. Abate, S. C. Glotzer, and D. J. Durian, Measurement of growing dynamical length scales and prediction of the jamming transition in a granular material, *Nature Physics* **3**, 260 EP (2007).
 - [16] R. Das, B. P. Bhowmik, A. B. Puthirath, T. N. Narayanan, and S. Karmakar, *Soft-pinning: Experimental validation of static correlations in supercooled molecular glass-forming liquids* (2021).
 - [17] A. Mutneja and S. Karmakar, Probing dynamic heterogeneity and amorphous order using rotational dynamics of rodlike particles in supercooled liquids, *Phys. Rev. Applied* **16**, 034022 (2021).
 - [18] A. Mutneja and S. Karmakar, Translational dynamics of a rod-like probe in supercooled liquids: an experimentally realizable method to study stokes-einstein breakdown, dynamic heterogeneity, and amorphous order, *Soft Matter* **17**, 5738 (2021).
 - [19] I. Chang, F. Fujara, B. Geil, G. Heuberger, T. Mangel, and H. Sillescu, Translational and rotational molecular motion in supercooled liquids studied by NMR and forced Rayleigh scattering, *Journal of Non-Crystalline Solids* **172**, 248 (1994).
 - [20] K. V. Edmond, M. T. Elsesser, G. L. Hunter, D. J. Pine, and E. R. Weeks, Decoupling of rotational and translational diffusion in supercooled colloidal fluids, *Proceedings of the National Academy of Sciences* **109**, 17891 (2012).
 - [21] F. R. Blackburn, C.-Y. Wang, and M. D. Ediger, Translational and rotational motion of probes in supercooled 1, 3, 5-tris(naphthyl)benzene, *The Journal of Physical Chemistry* **100**, 18249 (1996).
 - [22] S. A. Mackowiak, L. M. Leone, and L. J. Kaufman, Probe dependence of spatially heterogeneous dynamics in supercooled glycerol as revealed by single molecule microscopy, *Phys. Chem. Chem. Phys.* **13**, 1786 (2011).
 - [23] R. Zondervan, F. Kulzer, G. C. G. Berkhout, and M. Orrit, Local viscosity of supercooled glycerol near T_g probed by rotational diffusion of ensembles and single dye molecules, *Proceedings of the National Academy of Sciences* **104**, 12628 (2007).
 - [24] S. A. Mackowiak, T. K. Herman, and L. J. Kaufman, Spatial and temporal heterogeneity in supercooled glycerol: Evidence from wide field single molecule imaging,

- The Journal of Chemical Physics* **131**, 244513 (2009).
- [25] K. Paeng, H. Park, D. T. Hoang, and L. J. Kaufman, Ideal probe single-molecule experiments reveal the intrinsic dynamic heterogeneity of a supercooled liquid, *Proceedings of the National Academy of Sciences* **112**, 4952 (2015).
 - [26] C. Malinverno, S. Corallino, F. Giavazzi, M. Bergert, Q. Li, M. Leoni, A. Disanza, E. Frittoli, A. Oldani, E. Martini, T. Lendenmann, G. Deflorian, G. V. Beznoussenko, D. Poulikakos, K. H. Ong, M. Uroz, X. Trepas, D. Parazzoli, P. Maiuri, W. Yu, A. Ferrari, R. Cerbino, and G. Scita, Endocytic reawakening of motility in jammed epithelia, *Nature Materials* **16**, 587 (2017).
 - [27] R. Cerbino, S. Villa, A. Palamidessi, E. Frittoli, G. Scita, and F. Giavazzi, Disentangling collective motion and local rearrangements in 2d and 3d cell assemblies, *Soft Matter* **17**, 3550 (2021).
 - [28] K. E. Avila, H. E. Castillo, A. Fiege, K. Vollmayr-Lee, and A. Zippelius, Strong dynamical heterogeneity and universal scaling in driven granular fluids, *Phys. Rev. Lett.* **113**, 025701 (2014).
 - [29] L. M. C. Janssen, Active glasses, *J. Phys.: Condens. Matter* **31**, 503002 (2019).
 - [30] V. Narayan, S. Ramaswamy, and N. Menon, Long-lived giant number fluctuations in a swarming granular nematic, *Science* **317**, 105 (2007).
 - [31] L. F. Cugliandolo, G. Gonnella, and I. Petrelli, Effective temperature in active brownian particles, *Fluctuation and Noise Lett.* **18**, 1940008 (2019).
 - [32] L. Caprini, U. M. B. Marconi, C. Maggi, M. Paoluzzi, and A. Puglisi, Hidden velocity ordering in dense suspensions of self-propelled disks, *Phys. Rev. Res.* **2**, 023321 (2020).
 - [33] C. Merrigan, K. Ramola, R. Chatterjee, N. Segall, Y. Shokef, and B. Chakraborty, Arrested states in persistent active matter: Gelation without attraction, *Phys. Rev. Res.* **2**, 013260 (2020).
 - [34] S. Chaki and R. Chakraborty, Escape of a passive particle from an activity-induced energy landscape: emergence of slow and fast effective diffusion, *Soft Matter* **16**, 7103 (2020).
 - [35] S. K. Nandi, R. Mandal, P. J. Bhuyan, C. Dasgupta, M. Rao, and N. S. Gov, A random first-order transition theory for an active glass, *Proc. Natl. Acad. Sci. (USA)* **115**, 7688 (2018).
 - [36] G. Szamel, Theory for the dynamics of dense systems of athermal self-propelled particles, *Phys. Rev. E* **93**, 012603 (2016).
 - [37] S. K. Nandi, Activity-dependent self-regulation of viscous length scales in biological systems, *Phys. Rev. E* **97**, 052404 (2018).
 - [38] S. K. Nandi and N. S. Gov, Nonequilibrium mode-coupling theory for dense active systems of self-propelled particles, *Soft Matter* **13**, 7609 (2017).
 - [39] L. Berthier and J. Kurchan, Non-equilibrium glass transitions in driven and active matter, *Nat. Phys.* **9**, 310 (2013).
 - [40] K. Paul, S. K. Nandi, and S. Karmakar, Dynamic heterogeneity in active glass-forming liquids is qualitatively different compared to its equilibrium behaviour (2021), [arXiv:2105.12702 \[cond-mat.soft\]](https://arxiv.org/abs/2105.12702).
 - [41] K. Paul, S. K. Nandi, and S. Karmakar, *Non-trivial activity dependence of static length scale and critical tests of active random first-order transition theory* (2021).
 - [42] W. Kob and H. C. Andersen, Testing mode-coupling theory for a supercooled binary lennard-jones mixture i: The van hove correlation function, *Phys. Rev. E* **51**, 4626 (1995).
 - [43] M. Doi and S. F. Edwards, *The theory of polymer dynamics*, International series of monographs on physics No. 73 (Clarendon Press, Oxford, 2007).
 - [44] A. D. Parmar, S. Sengupta, and S. Sastry, Length-scale dependence of the stokes-einstein and adam-gibbs relations in model glass formers, *Physical Review Letters* **119**, 10.1103/physrevlett.119.056001 (2017).

A Novel Method to Probe the Pronounced Growth of Correlation Lengths in an Active Glass-forming Liquids using Elongated Probe

Supplementary Material

Anoop Mutneja ¹, and Smarajit Karmakar ¹

¹ *Tata Institute of Fundamental Research, 36/P,*

Gopanpally Village, Serilingampally Mandal,

Ranga Reddy District, Hyderabad, Telangana 500107, India

I. MODEL SYSTEM AND SIMULATION DETAILS

We simulated a binary glass-forming liquid known as the Kob-Andersen model [1]. The system contains the larger (A type) and smaller (B type) point particles in 80:20 ratio. This famous model mimics the $Ni_{80}P_{20}$ glass-forming liquids. The particles interact via potential,

$$V_{\alpha\beta}(\mathbf{r}) = 4\epsilon_{\alpha\beta} \left[\left(\frac{\sigma_{\alpha\beta}}{r} \right)^{12} - \left(\frac{\sigma_{\alpha\beta}}{r} \right)^6 \right] \quad (1)$$

Here α and β varies in the particle types, A, and B. The interaction strengths and the radii are $\epsilon_{AA} = 1.0$, $\epsilon_{AB} = 1.5$, $\epsilon_{BB} = 0.5$; $\sigma_{AA} = 1.0$, $\sigma_{BB} = 0.88$ and $\sigma_{AB} = 0.8$. The potential is truncated and smoothed upto second order derivative at $r = 2.5\sigma_{\alpha\beta}$. The units of length, energy, and time are defined in terms of the diameter of the larger particle (σ_{AA}), the pre-factor of the potential energy function (ϵ_{AA}), and $(\sqrt{m\sigma_{AA}^2\epsilon_{AA}})$, respectively, where $m = 1$ is the mass of the particle. We studied a system with $N = 50000$ particles, out of which $N_a = 0.1N$ of particles are chosen randomly to be active particles. These particles follow run-and-tumble motion with the persistence time of $\tau_p = 1.0$ in the Lennard-Jones unit. Physically each N_a particle would get an extra force $F_i^A = f_0(k_x^i\hat{x} + k_y^i\hat{y} + k_z^i\hat{z})$, with $k_{x,y,z}$ are randomly chosen from ± 1 , after every τ_p time. The system is studied in the temperature range $T \in [0.340 - 2.00]$, while the temperature is maintained via the Nosé-Hoover thermostat.

In each system, $N_r = 20$ probe rods are introduced and evolved via Newtonian dynamics. The rods consist of n_b number of beads (A-type) separated by a fixed distance of 0.3. These beads interact with other particles of the system via the same point potential and add up to the total force and torque of the rod. The n_b varies from 3 – 14, which would make the rod length in $L = 1.6 - 4.9$.

II. THE RELAXATION TIME, τ_α

Structural relaxation time, τ_α is defined as the time when the average value of overlap correlation $\langle Q(t) \rangle$ function drops to $1/e$ i.e. $\langle Q(\tau_\alpha) \rangle = 1/e$. The overlap correlation function at time t is the fraction of particles still left to move out of their cage length a . It is defined

as follows,

$$Q(t) = \frac{1}{N} \sum_{i=1}^N \theta(a - |\mathbf{r}_i(t) - \mathbf{r}_i(0)|) \quad (2)$$

where $\theta(x)$ is the usual step function and value of $a = 0.3$ is chosen to ignore the decorrelation that might happen due to vibrational motion of particles in their cages.

III. TRANSLATIONAL DIFFUSION CONSTANT, D_{cm}

The mean squared displacement (MSD) of CoM of the rod is defined as,

$$MSD = \langle |\mathbf{r}_{cm}(t) - \mathbf{r}_{cm}(0)|^2 \rangle = \langle |\Delta \mathbf{r}_{cm}|^2 \rangle, \quad (3)$$

where $\mathbf{r}_{cm}(t)$ is the CoM position vector at a time 't'. Translation diffusion constant (D_{cm}) for the CoM of the rod can be obtained from MSD using an expression $D_{cm}(T, L) = MSD(t \rightarrow \infty, T, L)/6t$.

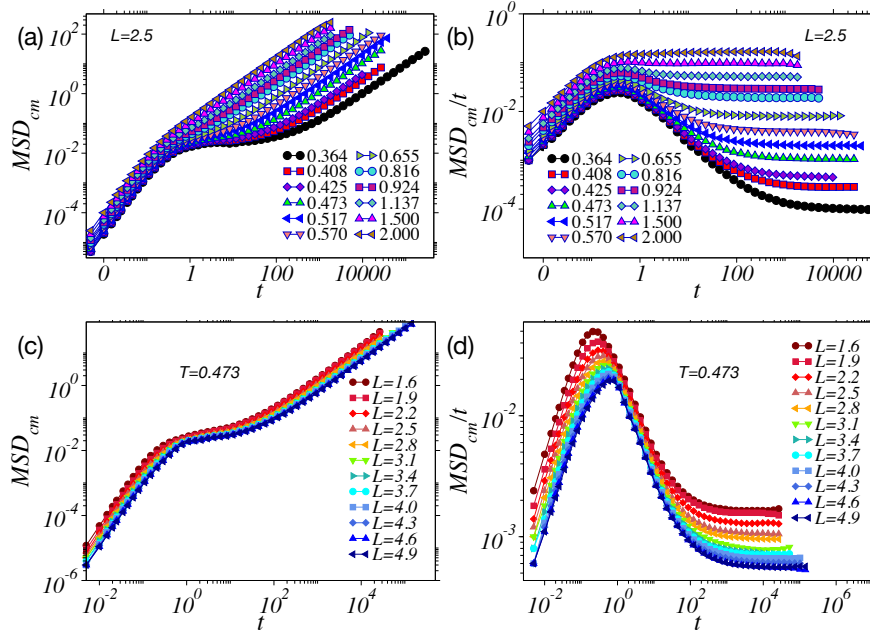


FIG. 1. (a) Mean squared displacements of CoM of rods of length $L = 2.5$ is shown for different parent liquids. Diffusion constant D_{cm} is calculated as the large time limit of MSD_{cm}/t . D_{cm} for a rod of length $L = 2.5$ immersed in supercooled liquid at different temperatures is shown in panel (b). The rod length dependence of the same can be seen in the lower panels, (c), and (d).

IV. TRANSLATIONAL RELAXATION TIME, τ_{cm}

The translational relaxation time is for CoM of the rod is chosen to be the time when on an average $1/e$ fraction of rods have displaced from their initial positions by a distance of $a = 0.3$, just like τ_α .

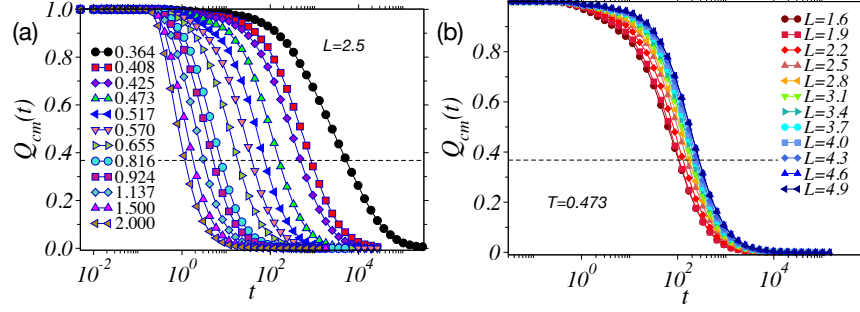


FIG. 2. (a) The overlap correlation function ($Q_{cm}(t)$) for CoM of the rod of length $L = 2.5$ subjected to different supercooling temperatures is shown. The time when averaged $Q_{cm}(t)$ drops to $1/e$ is taken to be the relaxation time (τ_{cm}) of the rod. (b) This panel shows variation in $Q_{cm}(t)$ with changing rod length.

V. ROTATIONAL RELAXATION TIME, τ_2^r

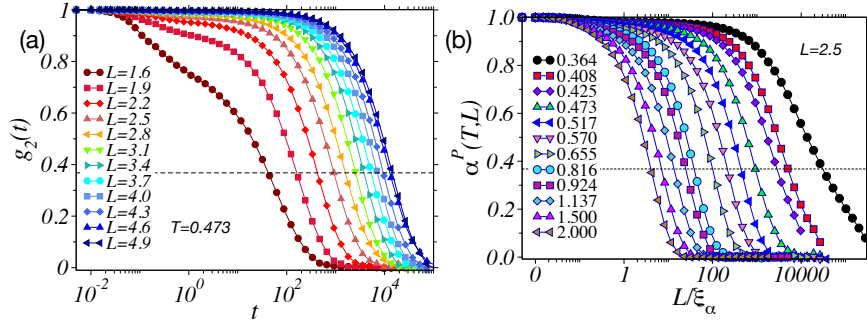


FIG. 3. (a) Rotational correlation function of rods of different lengths. (b) Rotational correlation function of rod subjected to various supercooling temperatures.

The rotational relaxation time is defined as the time when the second order rotational correlation function defined by the following expression decays to $1/e$.

$$g_2(t) = \langle P_2(\hat{u}(t) \cdot \hat{u}(0)) \rangle \quad (4)$$

Here, $\hat{u}(t)$ is the orientation vector of a rod at time ' t '.

VI. SUPERCOOLING EFFECTS ON ROD LENGTH DEPENDENCE OF TRANSLATIONAL RELAXATION TIME

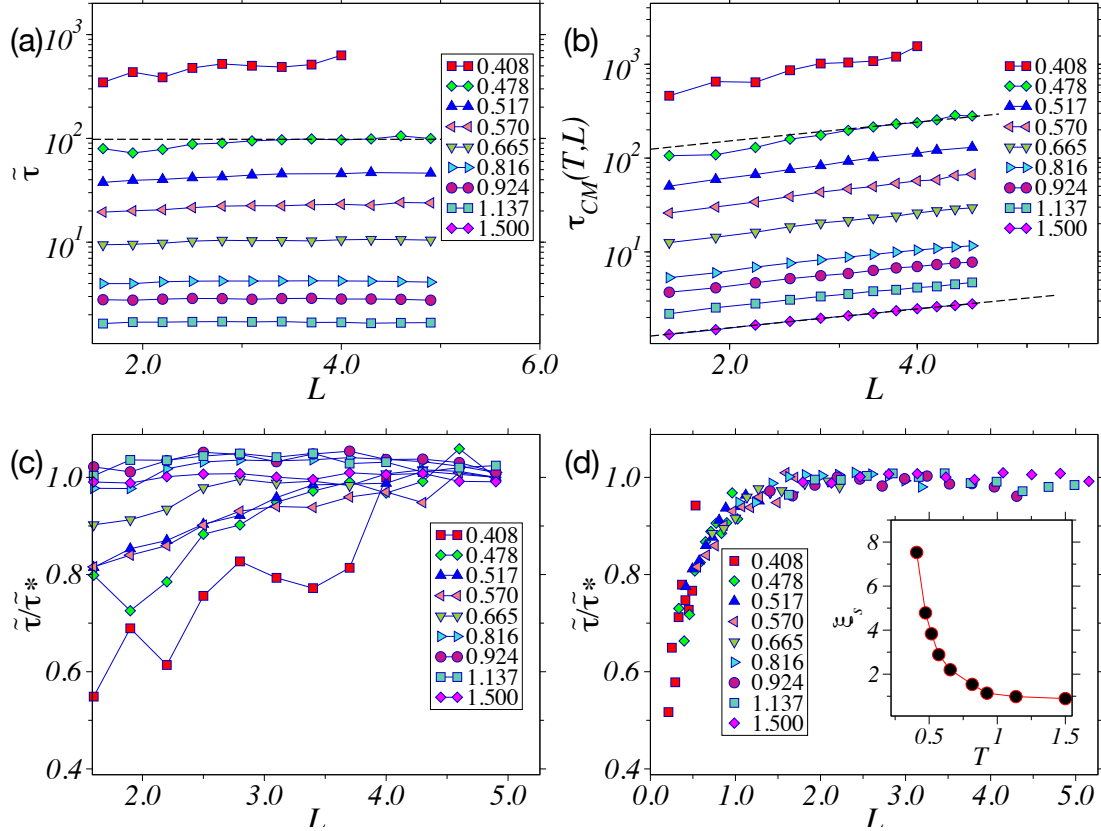


FIG. 4. (a) The rod length variation of the relaxation time of CoM of rod in system at different temperatures. The supercooling effects can be seen from the deviation from dotted lines ($\tau_{cm} \sim L/\ln(L/\sigma + b_2)$). (b) To quantify the deviation, $\tilde{\tau} = \tau_{cm} \ln(L/\sigma + b_2)/L$ is presented. (c) $\tilde{\tau}$ scaled by its large rod length limit, $\tilde{\tau}^*$ is plotted against the rod length. The variation clearly suggest the length scale involved. (d) Data collapse is shown by using the static length scale of the system. (used from ref.[2])

We successfully obtained the static length scale of the active supercooled liquid by studying the deviation of mean CoM diffusion constant from the known behaviour. It is already pointed out in the main text that the CoM diffusion constant and CoM relaxation time for rods are inversely related, implying both contains similar length scale information. In Fig.

4(a) we have shown the rod length dependence of τ_{cm} . For large temperature and large rod lengths, they follow the Brownian relation [3],

$$\tau_{cm} \sim \frac{L}{\ln(L/\sigma + b_2)}$$

. Here $\sigma = 1.0$ is the rod width, and, b_2 is constant to account for hydrodynamic interactions. It is evident from Fig. 4(a) that the shorter rods tend to move faster than expected from large rod length limit. To quantify the same we plotted $\tilde{\tau} = \tau_{cm} \ln(L/\sigma + b_2)/L$ in Fig. 4(b). In the next step to obtain the supercooling effect we scaled the $\tilde{\tau}$ by its large rod length limit in Fig. 4(c). The effect of supercooling for various sized rods is clearly different, signalling the involvement of an underlying length scale. The points in 4(c) are then collapsed to a master curve using the structural length scale reported in Ref. [2].

-
- [1] W. Kob and H. C. Andersen, [Phys. Rev. E **51**, 4626 \(1995\)](#).
 - [2] K. Paul, S. K. Nandi, and S. Karmakar, [Non-trivial activity dependence of static length scale and critical tests of active random first-order transition theory](#) (2021).
 - [3] M. Doi and S. F. Edwards, *The theory of polymer dynamics*, International series of monographs on physics No. 73 (Clarendon Press, Oxford, 2007).